

# Investigation of $\text{Fe}_3\text{O}_4$ /AEAP supermagnetic nanoparticles on the morphological, thermal and magnetite behavior of polyurethane rigid foam nanocomposites

Mir Mohammad Alavi Nikje<sup>1), \*),</sup> Maede Noruzian<sup>1)</sup>, Sahebeh Tamaddoni Moghaddam<sup>1)</sup>

DOI: dx.doi.org/10.14314/polimery.2015.026

**Abstract:** Novel, magnetic, polyurethane, rigid foam nanocomposites were synthesized by incorporation of surface modified iron oxide nanoparticles with *n*-(2-aminoethyl)-3-aminopropyltrimethoxysilane (AEAP) *via* a one shot method. The resulting data showed remarkable improvements in the thermal, as well as magnetic, properties of the nanocomposites when nanoparticles were incorporated into the polymer matrix. The prepared nanocomposites were characterized by Scanning Electron Microscopy (SEM), Fourier Transform Infrared Spectroscopy (FT-IR), Vibrating Sample Magnetometry (VSM), Thermo-mechanical Analysis (TMA) and Thermogravimetric Analysis (TGA). The effect of different amounts of  $\text{Fe}_3\text{O}_4$ /AEAP on the thermal and magnetic behavior of the resultant nanocomposite was investigated and the optimum percentage of the nanostructures in the foam formulation was defined.

**Keywords:** magnetic nanocomposite, polyurethane rigid foam, iron oxide, sol-gel method, surface functionalization.

## Wpływ dodatku supermagnetycznych nanocząstek $\text{Fe}_3\text{O}_4$ /AEAP na morfologię, termiczne i magnetyczne właściwości nanokompozytów sztywnych pianek poliuretanowych

**Streszczenie:** Nowe, magnetyczne nanokompozyty otrzymano metodą jednoetapową, wprowadzając do matrycy poliuretanowej (PUR) modyfikowane powierzchniowo nanocząstki żelaza ( $\text{Fe}_3\text{O}_4$ /AEAP). Badano wpływ dodatku różnej ilości nanocząstek magnetycznych na morfologię, właściwości termiczne i magnetyczne wytworzonych materiałów. Otrzymane sztywne pianki poliuretanowe zawierające cząstki  $\text{Fe}_3\text{O}_4$ /AEAP badano metodami skaningowej mikroskopii elektronowej (SEM), spektroskopii w podczerwieni z transformacją Fouriera (FT-IR), magnetometrii z wirującą próbką (VSM), analizy termomechanicznej (TMA) oraz termograwimetrycznej (TGA). Na podstawie uzyskanych wyników stwierdzono, że wprowadzone do matrycy poliuretanowej magnetyczne cząstki zmodyfikowanego tlenku żelaza wpłynęły korzystnie na termiczne i magnetyczne właściwości otrzymanych nanokompozytów sztywnych pianek poliuretanowych.

**Słowa kluczowe:** nanokompozyty magnetyczne, sztywne pianki poliuretanowe, tlenek żelaza, metoda zol-żel, funkcjonalizacja powierzchni.

Polyurethane (PUR) is one of the most versatile materials in the world today because of its wide application ranges from upholstered furniture, insulation in walls, roofs, biomaterials and thermoplastic PUR in medical devices and footwear, to coatings, adhesives, sealants and elastomers and automotive interiors [1, 2]. PUR has increasingly been used during the past thirty years in a variety of applications due to their comfort, cost benefits, energy savings and potential environmental soundness. Despite these extensive applications, PUR foams have some disadvantages *e.g.* low thermal stability and low

mechanical strengths. A great deal of effort has been devoted to overcoming these drawbacks by developing novel nanocomposite generations in recent years [3–5]. Incorporation of nanofiller into PUR foams leads to new applications for the nanocomposite. Recently, a synthetic method was reported incorporating silver nanoparticles (NPs) into PUR foams where the final nanocomposite was applied as an optical sensor [6]. In addition, Mohammadi and coworkers prepared magnetic PUR elastomer nanocomposites by incorporating pure and thiadiglycolic acid (TDGA) surface modified  $\text{Fe}_3\text{O}_4$  nanoparticles into a PUR matrix *via* an *in situ* polymerization method. Surface modification of  $\text{Fe}_3\text{O}_4$  nanoparticles allowed the preparation of magnetic nanocomposites with improved mechanical properties [7].

<sup>1)</sup> Imam Khomeini International University, Faculty of Science, Department of Chemistry, Qazvin, Iran, PO Box: 288.

<sup>\*</sup>) Author for correspondence; e-mail: drmm.alavi@gmail.com

Magnetic nanoparticles (MNPs) ( $\text{Fe}_3\text{O}_4$ ) show remarkable new phenomena such as super paramagnetism, high field irreversibility, high saturation field, extra anisotropy contributions or shifted loops after field cooling. The introduction of inorganic MNPs into polymer matrices can provide high-performance novel materials that find applications in many industrial fields and MNPs that provide high mechanical, thermal and magnetic properties are good candidates for the preparation of PUR nanocomposites. Nano scale magnetic materials have attracted considerable attention in recent years because of their potential applications in information storage, magnetic refrigeration, magneto-optical solid devices, cell separation and magnetic resonance imaging enhancement [8–10]. The interfacial interactions between the NPs and polymer matrix play a crucial role in determining the quality and properties of the nanocomposites. Understanding the interfacial interactions between the nanofiller and polymer matrix is important to improve the design and manufacture of polymer nanocomposites. It has been indicated that the formation of the  $\text{Fe}_3\text{O}_4$ /AEAP core-shell has some advantages such as less aggregation, supermagnetic properties, improvement of chemical stability, better dispersion in various matrices, stability at low pH, easy surface modification and easy control of the shell thickness in comparison with  $\text{Fe}_3\text{O}_4$  NPs [11]. The amino groups modified on the NP surfaces react with isocyanate to form urea linkages. A silica shell can be attached to MNPs *via* the Stöber method, which is based on the hydrolysis and condensation of a sol-gel precursor [12].

In the current study, an *in situ* polymerization method was used for the preparation of nanocomposites. The key to this approach is the distribution of nanofiller in the monomer. With control, the link between the nanofiller and the field material can achieve the desired distribution [13–16].

In this report, and in the continuation of our previous work on PUR magnetic nanocomposites [17], we sought to prepare PUR rigid foams with supermagnetic properties that can increase the functional application areas of PUR rigid foam and also improve some of its properties, such as low thermal stability. Nanocomposites were produced by an *in situ* method, whereas the MNPs and  $\text{Fe}_3\text{O}_4$ /AEAP core-shell were synthesized by co-precipitation and sol-gel methods, respectively. MNPs were used

at up to 3 % in the foam formulations and the thermal and magnetic properties of the nanocomposites were studied.

## EXPERIMENTAL PART

### Materials

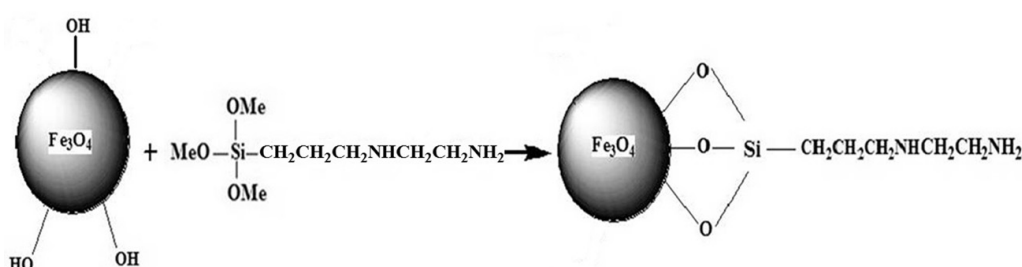
Dalto Foam TA® 14066 polyether polyol (OH NO. 430 ± 20, viscous yellow liquid, viscosity 526 Pa·s at 25 °C and water content 2.3 %) containing additives and methylene diphenyl diisocyanate (MDI) (Suprasec®5005, dark brown liquid, viscosity 22 Pa·s at 25 °C) for rigid PUR foam formulation were purchased from the Huntsman company and blown by the reaction of water with MDI. Iron(II) chloride tetrahydrate ( $\text{FeCl}_2 \cdot 4 \text{ H}_2\text{O}$ , 99.7 %), iron(III) chloride hexahydrate ( $\text{FeCl}_3 \cdot 6 \text{ H}_2\text{O}$ , 99.0 %), ammonia ( $\text{NH}_3 \cdot \text{H}_2\text{O}$ , 25–28 %), ethanol ( $\text{C}_2\text{H}_5\text{OH}$ , 99.7 %), *n*-(2-aminoethyl)-3-aminopropyltrimethoxysilane (AEAP) and citric acid were purchased from Merck and used as received without further purification.

### Synthesis of $\text{Fe}_3\text{O}_4$ /AEAP magnetic nanoparticles

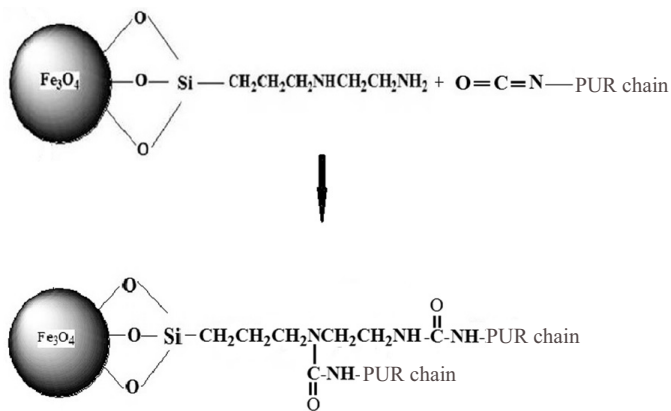
The super paramagnetic NPs were synthesized by a chemical co-precipitation method with ferric chloride and ferrous chloride (2/1 mol/mol) according to previous reports [18–20]. For the synthesis of  $\text{Fe}_3\text{O}_4$ /AEAP, at first 500 cm<sup>3</sup> of ethanol and 100 cm<sup>3</sup> of deionized water were placed into a round bottom flask, and then 500 mg of  $\text{Fe}_3\text{O}_4$  MNPs were added. The solution was sonicated for 20 min and then 2 cm<sup>3</sup> of AEAP was added. The reaction mixture was stirred mechanically at room temperature for 2 h. The resulting dark brown precipitation was washed 2 times with de-ionized water and dried at 50 °C in an oven for 24 h [21]. Scheme A shows the formation of  $\text{Fe}_3\text{O}_4$ /AEAP.

### Synthesis of the $\text{Fe}_3\text{O}_4$ /AEAP-PUR nanocomposites

Nanocomposites were synthesized by an *in situ* polymerization method. For the synthesis of the  $\text{Fe}_3\text{O}_4$ /AEAP nanocomposite, 0.05, 0.10, 0.15, 0.20, 0.25, and 0.30 g of MNPs were dispersed in polyol and the mixture sonicated for 4 min on an ultrasonic homogenizer (Hielscher, UP200S, Germany) to obtain significant dispersion. Then, the nanoparticulated polyol was hand mixed with MDI in



Scheme A



Scheme B

a  $300 \text{ cm}^3$  paper cup at 10:12 (polyol:MDI) ratios. Finally, the sample was kept at room temperature for 24 h for post curing and future testing [17]. The formation of PUR-riid foam nanocomposite is shown in Scheme B.

The prepared nanocomposites were labeled RPUR<sub>n</sub>, where (n) is the Fe<sub>3</sub>O<sub>4</sub>/AEAP percentages in the foam formulation.

### Methods of testing

- The morphology and particle size of the magnetite, Fe<sub>3</sub>O<sub>4</sub>/AEAP and PUR nanocomposite were studied by Field Emission Scanning Electron Microscopy (FE/SEM, Hitachi model SE 4160).

- FT-IR spectra were obtained on a Bruker Tensor 27 spectrophotometer.

- TGA was performed with a Perkin-Elmer Pyris Diamond.

- TGA/DTA was under an air atmosphere at a heating rate of  $7.5 \text{ }^\circ\text{C}/\text{min}$ .

- The Thermal Mechanical Analysis (TMA) measurements were performed with a thermal mechanical analyzer (LinseisTP-1000, Germany) over a temperature range of  $-100\text{--}250 \text{ }^\circ\text{C}$  and in compression mode.

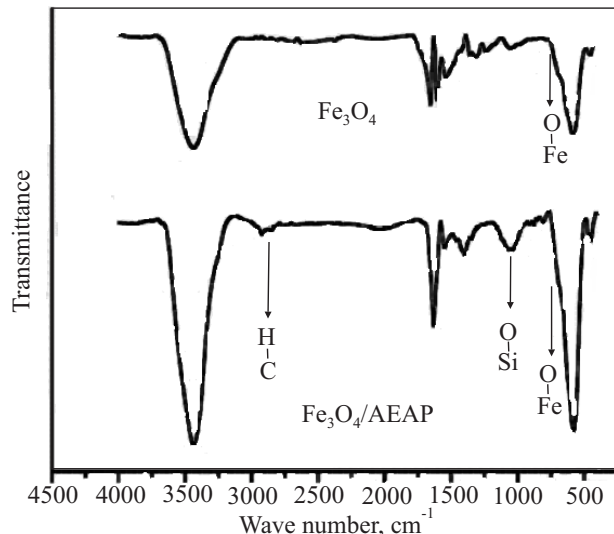
- The magnetic properties of the samples were studied using a vibrating sample magnetometer (VSM).

## RESULTS AND DISCUSSION

### Characterization of magnetite and Fe<sub>3</sub>O<sub>4</sub>/AEAP nanoparticles

#### Infrared spectroscopy

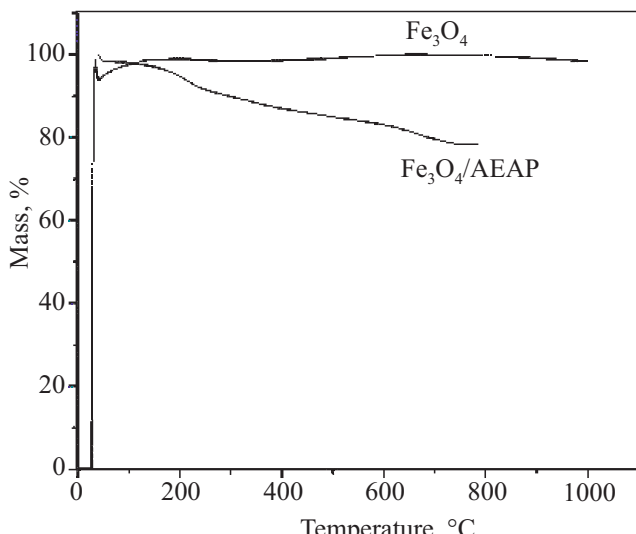
Functional groups were identified by recording the FT-IR spectra in the spectral range of  $400\text{--}4500 \text{ cm}^{-1}$ . As shown in Fig. 1, characteristic absorptions of Fe-O bonds are observed at  $491$  and  $595 \text{ cm}^{-1}$  due to bending and stretching, respectively. The presence of Fe-O-Si bonds cannot be seen in the FT-IR spectrum because they appear at around  $595 \text{ cm}^{-1}$  and therefore overlap with the Fe-O

Fig. 1. FT-IR spectra of Fe<sub>3</sub>O<sub>4</sub> and Fe<sub>3</sub>O<sub>4</sub>/AEAP

vibration of magnetite NPs [22, 23]. It can be seen in comparison with the unmodified sample, the modified Fe<sub>3</sub>O<sub>4</sub> nanoparticles possess an absorption band at  $1082 \text{ cm}^{-1}$  due to the Si-O stretching vibration [22]. The vibration bonds in the  $3300\text{--}3500 \text{ cm}^{-1}$  range are assigned to NH<sub>2</sub> group stretching vibrations. The absorption bands at  $2925$  and  $2970 \text{ cm}^{-1}$  are assigned to the stretching vibration of the C-H bond [24].

#### Thermogravimetric analysis

Figure 2 shows the TGA curves of Fe<sub>3</sub>O<sub>4</sub> and Fe<sub>3</sub>O<sub>4</sub>/AEAP NPs. The initial weight loss at  $40 \text{ }^\circ\text{C}$  in the Fe<sub>3</sub>O<sub>4</sub> curve is due to the removal of physically adsorbed solvent. The weight loss of AEAP modified MNPs (21 %) in the Fe<sub>3</sub>O<sub>4</sub>/AEAP curve can be seen at  $210 \text{ }^\circ\text{C}$ , which is due to the thermal decomposition of the *n*-(2-aminoethyl)-3-aminopropyltrimethoxysilane (AEAP) groups.

Fig. 2. TGA of Fe<sub>3</sub>O<sub>4</sub> and Fe<sub>3</sub>O<sub>4</sub>/AEAP NPs

### Scanning electron microscopy

FE-SEM was applied to characterize the size and morphology of the spherical MNPs. The size of uncoated spherical NPs and AEAP-coated NPs are 30–40 nm and 45–50 nm, respectively (Fig. 3). Also, it can be seen in Fig. 4 that the NPs are well distributed in the polymer matrix. These results show that little agglomeration of synthesized NPs takes place.

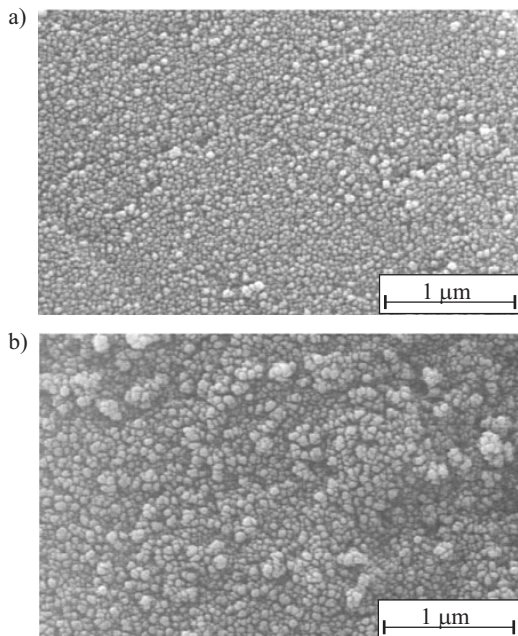


Fig. 3. FE-SEM images of: a)  $\text{Fe}_3\text{O}_4$ , b)  $\text{Fe}_3\text{O}_4/\text{AEAP}$  NPs

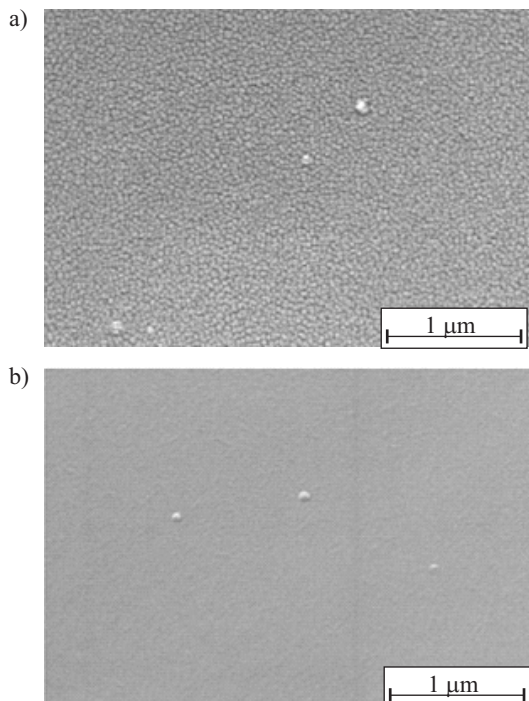


Fig. 4. FE-SEM images of distributed NPs in the PUR rigid foam:  
a) RPUR<sub>1.5</sub>, b) RPUR<sub>3.0</sub>

### Characterization of PUR-rigid foam nanocomposites

#### Infrared spectroscopy

Figure 5 shows the FT-IR results of  $\text{Fe}_3\text{O}_4/\text{AEAP}$ -PUR nanocomposite blending with different amounts of MNPs. As can be seen in these spectra, the stretching vibration at  $1100 \text{ cm}^{-1}$  is due to C-O bonds. The absorption band at  $1580 \text{ cm}^{-1}$  belongs to the N-H deformation vibration and C-N bond [25]. The absorption band at  $1730 \text{ cm}^{-1}$  is due to C=O stretching vibrations [26]. These spectra also show a characteristic peak of unreacted NCO groups at  $2273 \text{ cm}^{-1}$  [27]. The absorption bands at  $2860$  and  $2931$

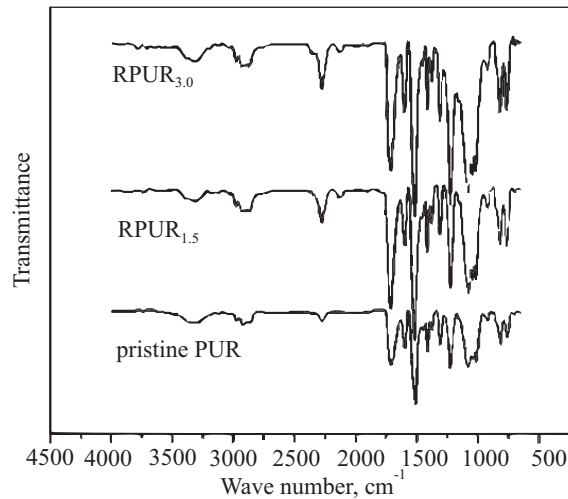


Fig. 5. FT-IR spectra of pure PUR and  $\text{Fe}_3\text{O}_4/\text{AEAP}$  filled PUR-rigid foams

$\text{cm}^{-1}$  are attributed to  $\text{CH}_2$  asymmetric stretching vibrations. A broad absorption band at  $3200$ – $3400 \text{ cm}^{-1}$  corresponds to the N-H stretching vibration [28]. As can be seen in Fig. 5, the samples containing 1.5 and 3.0 % nanofiller have strong absorptions that show a favored bonding between PUR chain bonds and  $\text{Fe}_3\text{O}_4/\text{AEAP}$ . This result indicates that crosslinking is increased.

#### Thermogravimetric analysis

Thermogravimetric analysis (TGA) is a profitable technique to determine the quantitative degradation based on the weight loss of a composite material as a function of temperature. The thermal stability of the samples was evaluated in initial ( $T_0$ ), 5 % ( $T_{5\%}$ ), 10 % ( $T_{10\%}$ ) and maximum ( $T_{max}$ ) temperatures [29, 30]. The temperature of the first degradation, about  $172^\circ\text{C}$ , was increased with higher amounts of NPs (Fig. 6). As shown in Table 1, the thermal degradation temperature values shift to higher temperatures with the addition of various percentages of NPs. In other words, the thermal resistance of PUR foams is increased. The possible reason for this behavior is attributed to reducing the PUR chain mobility [31]. Further-

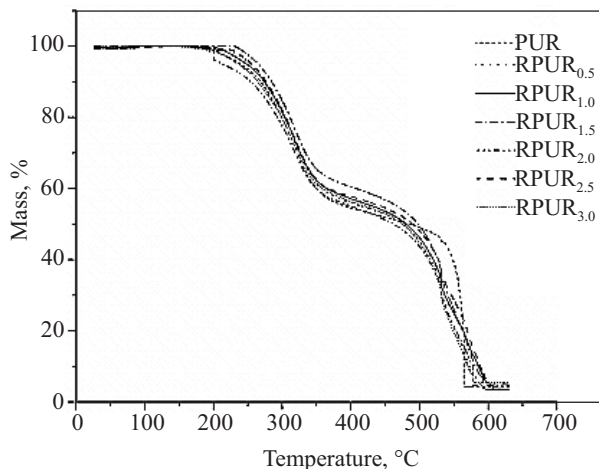


Fig. 6. TGA of pure PUR and  $\text{Fe}_3\text{O}_4/\text{AEAP}$  filled PUR-rigid foams

more, by increasing the  $\text{Fe}_3\text{O}_4/\text{AEAP}$  content in the polymer matrix, the formation of carbon residues are increased and this can explain the high heat capacity of  $\text{Fe}_3\text{O}_4/\text{AEAP}$  and its performance as a thermal insulator. The irregularities in thermal behavior with different amounts of filler can be explained as an inappropriate distribution of the nanoparticles that don't establish appropriate crosslinking between the polymer matrix and the amine functionalized NPs.

#### Scanning electron microscopy

FE-SEM images of the  $\text{Fe}_3\text{O}_4/\text{AEAP}$ -PUR nanocomposite are shown in Fig. 7. The shapes of the PUR rigid foam

**Table 1.** Degradation temperature of PUR rigid foam with various percentages of filler

Sample	$T_0$ , °C	$T_{5\%}$ , °C	$T_{10\%}$ , °C	$T_{max}$ , °C	Residue, %
PUR	172.59	219.14	253.42	565.29	3.53
RPUR <sub>0.5</sub>	197.84	261.06	283.97	553.60	3.57
RPUR <sub>1.0</sub>	203.10	248.77	278.85	565.23	4.12
RPUR <sub>1.5</sub>	205.53	213.94	254.79	566.73	3.76
RPUR <sub>2.0</sub>	202.05	258.61	293.25	543.03	4.21
RPUR <sub>2.5</sub>	212.64	262.92	283.98	569.11	4.64
RPUR <sub>3.0</sub>	210.52	236.96	265.34	569.30	5.56

cells are spherical. The spherical shaped cells are found to be closed cells. Figure 7 shows that the foams have a higher number of cells as the concentration of AEAP is increased. This indicates that a higher percentage of nanofiller reduces the cell size. A decrease in the cell size leads to a reduction in the heat transfer and improvement in the thermal insulation efficiency [32, 33]. According to SEM images (Fig. 7), and using equation (1), the cell density of the synthesized nanocomposite can be calculated (Table 2) [34]:

$$N_f = (nM^2/A)^{3/2} \quad (1)$$

In this formula,  $N_f$  (cells/cm<sup>3</sup>) is the cell density,  $n$  is the number of cells in a specific area of the SEM micrograph,  $A$  (cm<sup>2</sup>) is the area of the micrograph and  $M$  is the magnification factor of the SEM images, which is  $\times 40$  in this case.

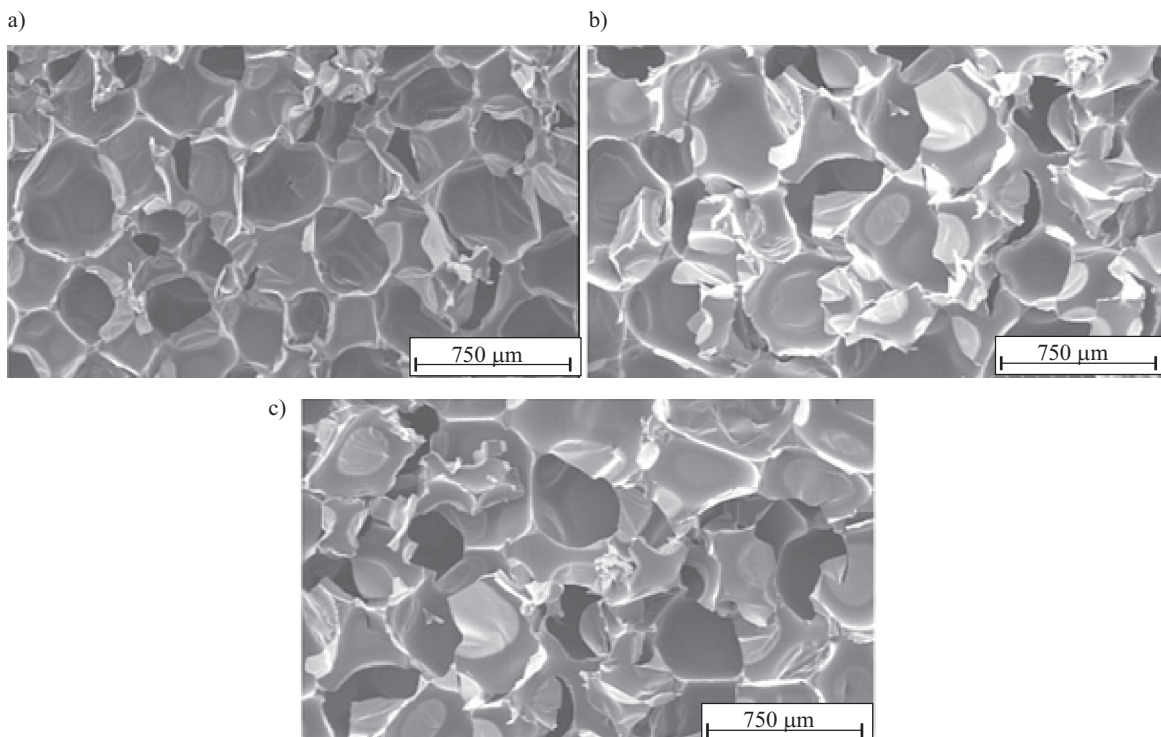


Fig. 7. FE-SEM images of PUR rigid foams modified with  $\text{Fe}_3\text{O}_4/\text{AEAP}$  NPs: a) PUR, b) RPUR<sub>1.5</sub>, c) RPUR<sub>3.0</sub>

**T a b l e 2.** Cell density of nanocomposite foams based on  $\text{Fe}_3\text{O}_4/\text{AEAP}$  NPs

Sample	PUR	RPUR <sub>1.5</sub>	RPUR <sub>3.0</sub>
$N_f(\text{cells}/\text{cm}^3) \cdot 10^5$	0.84	0.52	0.78

The foam density of the synthesized nanocomposites (Fig. 8) is calculated according to equation 2:

$$D = (M/V) \quad (2)$$

where:  $D (\text{g}/\text{cm}^3)$  — the foam density,  $M (\text{g})$  — the weight,  $V (\text{cm}^3)$  — the volume of the sample. As can be seen in Fig. 8, incorporation of filler increases the foam density.

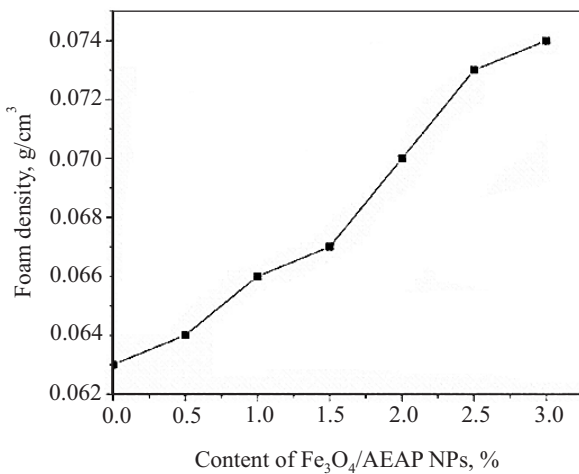


**Fig. 8.** Foam density of RPUR nanocomposites based on  $\text{Fe}_3\text{O}_4/\text{AEAP}$  NPs

### Magnetic properties

The magnetic properties of  $\text{Fe}_3\text{O}_4/\text{AEAP}$ -PUR nanocomposite with 1.5 and 3.0 % nanofiller were characteri-

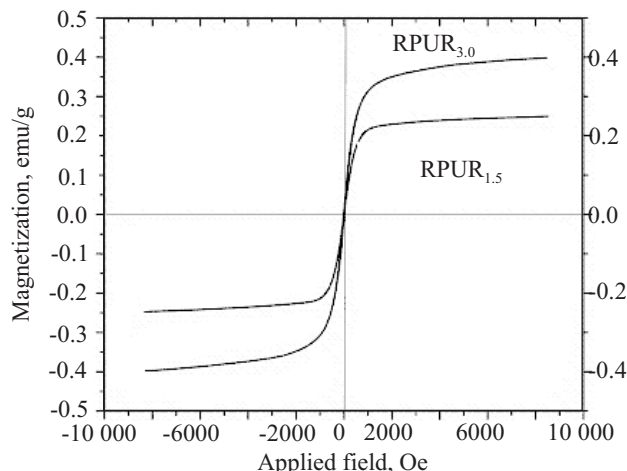


**Fig. 9.** Hysteresis loops by VSM of the PUR rigid foam nanocomposite modified with  $\text{Fe}_3\text{O}_4/\text{AEAP}$  NPs

zed by vibrating sample magnetometry (VSM). The supermagnetic property of the 1.5 and 3.0 % nanocomposites are about 0.25 and 0.41 emu/g, respectively. As can be seen in Fig. 9, the resultant nanocomposite was shown to possess superparamagnetic behavior at room temperature as no hysteresis loop was observed in the magnetization graph. Also, the remanence and coercivity in the absence of the external field were zero.

### TMA studies

The linear thermal expansion coefficient ( $\alpha$ ) and the glass transition temperature ( $T_g$ ) are parameters that can be extracted from TMA graphs. The softening point of foams is the temperature where the sample shows a severe decline in its dimensions. As can be seen in Fig. 10,  $T_g$  is decreased with an increase in the MNPs content in

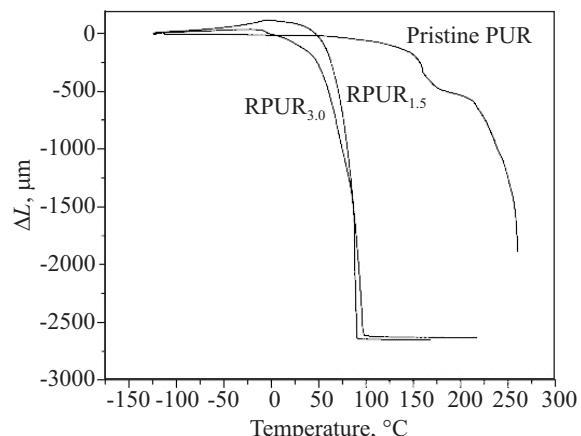


**Fig. 10.** TMA of pure PUR and RPUR nanocomposites

the foam. The reason for this behavior is assigned to the placement of modified NPs in between the PUR chains and thus a reduction in the direct crosslinking degree between PUR chains and also enhancing the soft segment mobility [17]. Furthermore, an increment in the  $\alpha$  value in the nanocomposite samples is confirmed with a dimensional instability and reduction in elastic properties of the cell walls.

### CONCLUSIONS

MNPs ( $\text{Fe}_3\text{O}_4$ ) and AEAP-coated MNPs with 35 and 45 nm average diameter were prepared by co-precipitation and sol-gel method, respectively. It has been shown that AEAP-coated MNPs can significantly improve the thermal properties of PUR. This type of inorganic NP is chemically trapped in a PUR matrix by the formation of hydrogen bonds between the urea linkages. The NPs are well distributed up to 3.0 % in the PUR polymer matrix and with this increase, the thermal resistance of the foam, and also the amount of remaining char, were increased.

$T_g$  reduced in nano-filled PUR rigid foams. In addition, the resultant nanocomposites were shown to have supermagnetic behavior.

## REFERENCES

- [1] Zia K.M., Bhatti H.N., Ahmad Bhatti I.: *React. Funct. Polym.* **2007**, *67*, 675. <http://dx.doi.org/10.1016/j.reactfunctpolym.2007.05.004>
- [2] Silvestri A., Serafini P.M., Sartori S., Ferrando P., Boccafoschi F., et al.: *Appl. Polym. Sci.* **2011**, *122*, 3661. <http://dx.doi.org/10.1002/app.34779>
- [3] Fan H., Tekeei A., Suppes G. J., Hsieh F. H.: *Appl. Polym. Sci.* **2013**, *127*, 1623, <http://dx.doi.org/10.1002/app.37508>
- [4] Choi J., Kim D., Ryu K., Lee H. I., Jeong H., Shin C., Kim J., Kim B.: *Macromol. Res.* **2011**, *19*, 809. <http://dx.doi.org/10.1007/s13233-011-0801-4>
- [5] Pei A., Malho J.M., Ruokolainen J., Zhou Q., Berglund L.A.: *Macromolecules* **2011**, *44*, 4422. <http://dx.doi.org/10.1021/ma200318k>
- [6] Apyari V.V., Volkov P.A., Dmitrienko S.G.: *Adv. Nat. Sci.: Nanosci. Nanotechnol.* **2012**, *3*, 015001. <http://dx.doi.org/10.1088/2043-6262/3/1/015001>
- [7] Mohammadi A., Barikani M., Barmar M.: *Mater. Sci.* **2013**, *48*, 7493. <http://dx.doi.org/10.1007/s10853-013-7563-7>
- [8] Akbarzadeh A., Samiei M., Davaran S.: *Nanoscale. Res. Lett.* **2012**, *7*, 144. <http://dx.doi.org/10.1186/1556-276X-7-144>
- [9] Batlle X., Perez N., Guardia P., Iglesias O., Labarta A., et al.: *Appl. Phys.* **2011**, *109*, 07B524. <http://dx.doi.org/10.1063/1.3559504>
- [10] Du G.H., Liu Z.L., Xia X., Chu Q., Zhang S.M.: *Sol-Gel Sci. Technol.* **2006**, *39*, 285. <http://dx.doi.org/10.1007/s10971-006-7780-5>
- [11] Ahangaran F., Hassanzadeh A., Nouri S.: *Int. Nano Lett.* **2013**, *3*, 23. <http://dx.doi.org/10.1186/2228-5326-3-23>
- [12] Emadi M., Shams E., Amini M.K.: *J. Chem.* **2013**, *2013*, *10*. <http://dx.doi.org/10.1155/2013/787682>
- [13] Guo Z., Kim T.Y., Lei K., Pereira T., Sugar J.G., Hahn H.T.: *Compos. Sci. Technol.* **2008**, *68*, 164. <http://dx.doi.org/10.1016/j.compscitech.2007.05.031>
- [14] Kotal M., Srivastava S.K., Manu S.K., Saxena A.K., Pandey K.N.: *Polym. Int.* **2013**, *62*, 728. <http://dx.doi.org/10.1002/pi.4354>
- [15] Milani M.A., González D., Quijada R., Basso N.R.S., Cerrada M.L., et al.: *Compos. Sci. Technol.* **2013**, *84*, 1. <http://dx.doi.org/10.1016/j.compscitech.2013.05.001>
- [16] Sahoo N.G., Rana S., Cho J.W., Li L., Chan S.H.: *Prog. Polym. Sci.* **2010**, *35*, 837. <http://dx.doi.org/10.1016/j.progpolymsci.2010.03.002>
- [17] Alavi Nikje M.M., Farahmand Nejad M.A., Shabani K., Haghshenas M.: *Colloid Polym. Sci.* **2013**, *291*, 903. <http://dx.doi.org/10.1007/s00396-012-2808-6>
- [18] Ahn T., Kim J.H., Yang H.M., Lee J.W., Kim J.D.: *Phys. Chem. C* **2012**, *116*, 6069. <http://dx.doi.org/10.1021/jp211843g>
- [19] Mendoza-Bello S., Morales-Luckie R., Flores-Santos L., Hinestroza J., Sanchez-Mendieta V.: *Nanopart. Res.* **2012**, *14*, 1242. <http://dx.doi.org/10.1007/s11051-012-1242-5>
- [20] Wu S., Sun A., Zhai F., Wang J., Xu W., Zhang Q., Volinsky A.A.: *Mater. Lett.* **2011**, *65*, 1882. <http://dx.doi.org/10.1016/j.matlet.2011.03.065>
- [21] Ma M., Zhang Y., Yu W., Shen H.Y., Zhang H.Q., Gu N.: *Colloids Surf. A: Physicochem. Eng. Asp.* **2003**, *212*, 219. [http://dx.doi.org/10.1016/S0927-7757\(02\)00305-9](http://dx.doi.org/10.1016/S0927-7757(02)00305-9)
- [22] Feng B., Hong R.Y., Wang L.S., Guo L., Li H.Z., et al.: *Colloids Surf. A: Physicochem. Eng. Asp.* **2008**, *328*, 52. <http://dx.doi.org/10.1016/j.colsurfa.2008.06.024>
- [23] Kassaee M., Masrouri H., Movahedi F.: *Appl. Catal. A: Gen.* **2011**, *395*, 28. <http://dx.doi.org/10.1016/j.apcata.2011.01.018>
- [24] Zhou L., Li G., An T., Li Y.: *Res. Chem. Intermed.* **2010**, *36*, 277. <http://dx.doi.org/10.1007/s11164-010-0134-5>
- [25] Sriram V., Sundar S., Dattathereyan A., Radhakrishnan G.: *React. Funct. Polym.* **2005**, *64*, 25. <http://dx.doi.org/10.1016/j.reactfunctpolym.2005.04.005>
- [26] Tsai M.H., Huang S.L., Liu S.J., Chen C.J., Chen P.J., Chen S.H.: *Desalination* **2008**, *233*, 191. <http://dx.doi.org/10.1016/j.desal.2007.09.042>
- [27] Narine S., Kong X., Bouzidi L., Sporns P.: *Amer. Oil. Chem. Soc.* **2007**, *84*, 65. <http://dx.doi.org/10.1007/s11746-006-1008-2>
- [28] Wang Z., Zhou Y., Sun Y.: *J. Inorg. Organomet. Polym.* **2009**, *19*, 202. <http://dx.doi.org/10.1007/s10904-008-9234-8>
- [29] Mythili C.V., Retna A.M., Gopalakrishnan S.: *Bull. Mater. Sci.* **2004**, *27*, 235. <http://dx.doi.org/10.1007/BF02708512>
- [30] Zammarano M., Krämer R.H., Harris R., Ohlemiller T.J., Shields J.R., et al.: *Polym. Adv. Technol.* **2008**, *19*, 588. <http://dx.doi.org/10.1002/pat.1111>
- [31] Bikaris D.: *Thermochimica Acta* **2011**, *523*, 1. <http://dx.doi.org/10.1016/j.tca.2011.06.010>
- [32] Prociak A., Pielichowski J., Sterzynski T.: *Polym. Test.* **2000**, *19*, 705. [http://dx.doi.org/10.1016/S0142-9418\(99\)00042-2](http://dx.doi.org/10.1016/S0142-9418(99)00042-2)
- [33] Tang Z., Maroto-Valer M.M., Andrésen J.M., Miller J.W., Listemann M.L., et al.: *Polym.* **2002**, *43*, 6471. [http://dx.doi.org/10.1016/S0032-3861\(02\)00602-X](http://dx.doi.org/10.1016/S0032-3861(02)00602-X)
- [34] Han X., Zeng C., Lee L.J., Koelling K.W., Tomasko D.L.: *Polym. Eng. Sci.* **2003**, *43*, 1261. <http://dx.doi.org/10.1002/pen.10107>

Received 12 XI 2013.